

Topological origin of subgap conductance in insulating bilayer graphene

Jian Li,¹ Ivar Martin,² Markus Büttiker,¹ and Alberto F. Morpurgo³

¹Département de Physique Théorique,

Université de Genève, CH-1211 Genève 4, Switzerland

²Theoretical Division, Los Alamos National Laboratory,

Los Alamos, New Mexico 87545, USA

³DPMC and GAP, Université de Genève, CH-1211 Genève 4, Switzerland

(Dated: March 26, 2010)

The edges of graphene-based systems possess unusual electronic properties, originating from the non-trivial topological structure associated to the spinorial character of the electron wave-functions. These properties, which have no analogue for electrons described by the Schrödinger equation in conventional systems, have led to the prediction of many striking phenomena, such as gate-tunable ferromagnetism and valley-selective transport [1–3]. In most cases, however, the predicted phenomena are not expected to survive the influence of the strong structural and chemical disorder that unavoidably affects the edges of real graphene devices. Here, we present a theoretical investigation of the intrinsic low-energy states at the edges of electrostatically gapped bilayer graphene (BLG), and find that the contribution of edge modes to the conductance of realistic devices remains sizable even for highly imperfect edges. This edge conductance dominates over the bulk contribution if the electrostatically induced gap is sufficiently large, and accounts for seemingly conflicting observations made in recent transport and optical spectroscopy experiments [4–6]. Our results illustrate the robustness of phenomena whose origin is rooted in the topology of the electronic band-structure, even in the absence of specific protection mechanisms.

The electronic structure of graphene single- and bi-layers possesses nontrivial topological properties, which originate from the spinorial nature of the electronic wave-functions, and that manifest themselves in many ways. For instance, when transported along a closed trajectory, the wave-function of an electron in single- or bi-layer graphene acquires a non-vanishing Berry phase, responsible for the specific quantization sequence of the Hall conductance that is observed experimentally [7–9]. Another manifestation of the topological properties is the presence of zero-energy states living at the material edges [10–12]. The existence of these states is allowed by the richer structure of edge boundary conditions (as compared to the conventional scalar wave-functions) that is associated to the spinorial nature of the electronic wave-functions (see, e.g., [13]).

Many fascinating phenomena originating from the properties of edge states in graphene layers have been predicted theoretically, such as electric-field tunable magnetism [1] and valley-dependent transport [2, 3]. In most cases, however, the possibility to observe these phenomena is dubious, because theory often relies on a perfectly ordered atomic structure

of the graphene edges, whereas in real materials strong disorder is unavoidably present. To examine if exotic aspects of the edge physics can survive disorder, here we analyze the transport properties of low-energy edge states in the case of gapped BLG [14]. Contrary to the naive expectation, we show that transport mediated by the low-energy edge states exhibits universal features, and persists even in the presence of very strong disorder.

To illustrate the topological origin of edge states in gapped BLG (Fig. 1a) we describe the low-energy electronic properties of this material in terms of an effective (dimensionless) Hamiltonian, by now well-established both theoretically and experimentally [14]:

$$H_\tau = -\mathbf{g}_\tau(k_x, k_y) \cdot \boldsymbol{\sigma}, \quad (1)$$

$$\mathbf{g}_\tau(k_x, k_y) = (k_x^2 - k_y^2, 2k_x k_y \tau, \Delta),$$

where $\boldsymbol{\sigma}$ stands for the vector of Pauli matrices, $\tau = \pm 1$ indexes the two valleys in the band-structure (corresponding to the K and K' points in the Brillouin zone), $\mathbf{k} = (k_x, k_y)$ is the momentum relative to the K/K' point, and 2Δ defines the size of the gap. This Hamiltonian – which can be derived as a long-wavelength low-energy limit of a tight-binding description – acts on spinors, whose components correspond approximately to the amplitude of the wave-function on atoms A1 and B2 of the bilayer unit cell (see Supporting Information for details). The non-trivial topological properties of BLG are described by the topological charge [15, 16]

$$c_\tau = \frac{1}{4\pi} \int dk_x \int dk_y \hat{\mathbf{g}}_\tau \cdot \left(\frac{\partial \hat{\mathbf{g}}_\tau}{\partial k_x} \times \frac{\partial \hat{\mathbf{g}}_\tau}{\partial k_y} \right), \quad (2)$$

which characterizes the mapping from a the region of the Brillouin zone that contains the valley point K/K' to the unit vector \mathbf{g}_τ defining the single-valley Hamiltonian. The topological charge c_τ equals 1 in one of the valleys and -1 in the other. From the bulk–edge correspondence [17, 18], it can then be expected that zero-energy states, propagating in opposite directions in the two valleys, appear at the material edge as a consequence of the discontinuity of the topological charge between BLG and vacuum. Indeed, “valley-helical” states appear at interfaces separating regions of BLG where the gap has opposite polarity [16], and have been shown to exist at zig-zag edges by Castro *et al.* [11] (Note that the latter authors based their analysis on the full tight-binding description of graphene, but the same states can be found in terms of the continuum low-energy Hamiltonian (1); see Fig. 1b and Supporting Information). In a device consisting of a strip of BLG with zig-zag edges, these zero-energy states propagate ballistically and are responsible for a finite conductance equal

to $4e^2/h$ (corresponding to two spin degenerate states at each one of the device edges) when the Fermi level is located inside the gap.

These properties of BLG parallel those of spin-orbit induced topological insulators [18–21], in which ballistic helical edge states have been observed experimentally [22, 23], but with the valley quantum number playing the role of the electron spin. A complete analogy between BLG and spin-orbit induced topological insulators, however, is prevented by a number of important differences. Most crucially, edge states in spin-orbit induced topological insulators cannot back-scatter (and hence do not localize) as long as time reversal symmetry is present – a phenomenon referred to as topological protection [19–21]. In graphene bilayers, on the other hand, any mechanism coupling states in different valleys can affect the edges states, since intervalley scattering is equivalent (in our analogy) to spin-flip processes for spin-orbit induced topological insulators. For instance, at an ideal armchair edge where the valleys are coupled by the boundary conditions [13], the zero-energy edge states are absent. For the same reason, it might be expected that any source of short range scattering due to the edge non-ideality will have the same effect, making the behavior found for ideal zig-zag edges irrelevant for the description of transport in real devices.

To analyze the properties of the low-energy states present at disordered edges we go back to the tight-binding description of gapped BLG, and perform numerical calculations of conductance for strips of gapped BLG. Short-range disorder is introduced in two different ways, which model different physical phenomena occurring at real graphene edges. Structural edge disorder is generated by removing randomly tight-binding sites in the two layers [24], up to a depth d from the starting edge (see examples in Fig. 1c and d). The effect of generic chemical species binding to the outermost carbon atoms is modeled by adding to the corresponding sites in the tight-binding Hamiltonian an energy that is distributed randomly in the range ± 1 eV (i.e., the characteristic order of magnitude associated to chemical bonds). We perform calculations starting from different “ideal” edges, including zig-zag, armchair, and other edges generated by cutting the BLG along arbitrary crystallographic directions, for many different microscopic realization of disorder, from which we extract the ensemble-averaged conductance. In the calculations, we use the known values for the in- and out-of-plane hopping parameters of BLG, and gap values in the range that is accessible to experiments (see Methods Section).

The ensemble-averaged conductance calculated as a function of sample length L for dif-

ferent values of d is shown in Fig. 2a and b, corresponding to the cases of starting ideal zig-zag and armchair edges, respectively. It is apparent that in all cases the average conductance decays exponentially with L . The calculated conductance is independent of the width W of the graphene strip, indicating that transport is indeed occurring along the edges (see Fig. 2d). Only for very short strips ($L < 5$ nm), a sizable “bulk” contribution to the conductance (scaling linearly with the width of the strip) is also significant, due to direct tunneling under the gap. This contribution decays very rapidly with increasing the device length, and can be neglected in the range of values of L that we are considering. Note also that the conductance calculated for large values of L extrapolates in all cases to $4e^2/h$ for $L \rightarrow 0$, as expected for edge transport (the factor 4 accounts for two edges and two spin directions). Therefore, the observed exponential decay of G as a function of L enables us to directly extract the localization length λ_{loc} of the edge states.

When starting from an ideal zig-zag edge, structural disorder causes localization of the pre-existing zero-energy states, and the observed decrease of λ_{loc} with increasing d is expected (see Fig. 3; the case where only structural disorder is considered corresponds to the points connected by the continuous line). Unexpectedly, however, we find that for strong disorder the localization length tends to saturate to a rather large value, that depends only on the magnitude of the gap (see Fig. 3 inset). The same behavior is observed when starting from other periodic edges, obtained by cutting the BLG lattice along different crystallographic directions. The situation is different when starting from an ideal armchair edge, as in that case we observe that both the conductance and localization length increase upon increasing the disorder strength. The increase occurs because for an ideal armchair edge no states exist in the gap, and disorder introduces low-energy states at the edges that mediate transport. Remarkably, also in this case, at large disorder strength the localization length saturates to the value found for disordered zig-zag edges. When chemical disorder is also included (see Fig. 2c and points connected by the broken line in Fig. 3), the localization length saturates in all cases again to the same universal value, already for a very small amount of structural disorder ($d = 1$). Physically, this implies that in the presence of sufficiently strong disorder there is no relation between the structure of the starting (ideal) edge and the low-energy electronic properties. In other words, our calculations show that in the presence of sufficient disorder, may it be structural or chemical, the electronic properties of graphene edges are universal, and they support low-energy electronic states responsible for sub-gap conduction.

Finding that low-energy sub-gap edge states – with a very long localization length given the large strength of disorder considered – are present and characterized by universal properties is remarkable. To highlight the importance of the band structure topology in the case of gapped BLG with disordered edges, we have performed numerical calculations on a gapped half-filled square lattice (see Fig. 4a), which, similarly to BLG, is bipartite, i.e., it is formed by two interpenetrating (square) sublattices. A gap in the electronic spectrum can be opened by unbalancing the sublattice energies (see Supporting Information; we used values for the tight-binding hopping amplitude and for the gap comparable to those of graphene). Despite superficial similarity, unlike in BLG, the resulting band structure is topologically trivial. Accordingly, intra-gap states are neither expected nor observed numerically at the ideal edges. Indeed, we find that for the square lattice, transport in the ideal case is due to weak direct tunneling under the gap. Edge roughness does not introduce edge states inside the gap, but only further suppresses conductance (see Fig. 4b and c). This comparison underscores the fundamental importance of the topological origin of low-energy edge states in gapped BLG. Even though these edge states are not protected against short-range potential scattering, as in the case for spin-orbit induced topological insulators [19, 21], their robustness manifests itself in a very long and universal localization length.

Having established that the presence of low-energy edge states with long localization length is a generic property of gapped BLG, we discuss how these states manifest in transport experiments. In this regard, the ability to tune the gap in BLG electrostatically up to values of ≈ 300 meV [5, 6] is particularly useful. For large gap values, hopping through localized states is expected to be the dominant low-temperature transport mechanism. Since the states localized at the edge naturally exist near the middle of the gap, they will give a dominant contribution to the measured conductance, as long as the potential fluctuations due to the bulk disorder are significantly smaller than the bulk gap. In real devices this condition is satisfied when the gap is sufficiently larger than the root mean square of potential fluctuations in the bulk, which for samples on SiO₂ substrate has been measured to be approximately 20 meV [25, 26]. To compare with experiments, we estimate the characteristic energy scale that determines the temperature dependence of the conductance. To this end, we assume that transport is dominated by variable range hopping along the edges (one dimensional transport; the case of nearest neighbor hopping would give a comparable result). The temperature dependence of the conductance can then be written in the form

$G \propto \exp[-(T^*/T)^{1/2}]$, with $T^* \approx V_g t a / (t_\perp \lambda_{loc})$ (see Supporting Information; here we have denoted the band-gap 2Δ with V_g , to emphasize that in the experiments this parameter can be controlled, and is proportional to the voltage applied between the gates). Therefore, T^* is the characteristic energy scale that determines the low temperature transport behavior: like the band gap, it increases with the applied gate voltage but it is approximately one order of magnitude smaller for the practically relevant values of V_g .

The dominating contribution of the edge states to the conductance resolves an apparent experimental controversy, namely that the energy scale commonly observed in the dc transport experiments [4] is significantly smaller than the bulk band gap expected theoretically or measured directly by optical spectroscopy [5, 6]. Indeed, in their study of the insulating state of electrostatically gapped BLG Oostinga *et al* [4] extracted a characteristic transport energy scale of about 5-10 meV, whereas the largest perpendicular electric field applied in that experiment corresponded to a band-gap of approximately 100-120 meV (as it can be inferred from the optical spectroscopy work performed later [5, 6]). Very recently, similar experiments have also been successfully performed on suspended, double-gated BLG (i.e., with the bulk of the bilayer not affected by the direct contact with other materials) [27]. In that case the maximum gap that could be opened electrostatically was estimated to be approximately 5 meV, while the resistance measured in dc transport exhibited an insulating behavior with an activation energy of 0.3 meV. For both experiments, the difference between expected bulk gap and characteristic energy scale measured in transport is about one order of magnitude, consistent with our analysis. The fact that, experimentally, agreement is found irrespective of whether the bilayer is in contact with a substrate or suspended indicates that the observed sub-gap transport is not likely to be caused by the bulk disorder. We therefore conclude that existing experiments do indeed support the scenario presented here, namely that sub-gap transport is dominated by conductance at the edges of the graphene bilayer.

It is quite surprising that low-energy edge states in gapped BLG survive – and dominate transport – even in the presence of very strong disorder, even though the topological protection mechanisms, which operate in the spin-orbit induced topological insulators, are absent. This finding illustrates the robustness of phenomena rooted in the underlying bulk band-structure topology, whose broad importance for condensed matter physics is starting to be fully appreciated only now. A unique feature of BLG is that, by using gate electrodes to control the magnitude and sign of the gap between valence and conductance band [16],

this underlying topology can be manipulated experimentally in nano-electronic devices.

Methods The rough edges of BLG samples in our simulations are generated by random walks (forward only) near the sample boundaries up to depth d , and 1000 random configurations are averaged for each data point. The calculations are always done at $E_f = 0$ for the samples, with highly doped contacts. The two-terminal conductance is calculated by using the recursive Green's function method, and the local density of states is obtained from the spectral function. The important parameters for the BLG samples, unless otherwise specified, are: $t = 2.8\text{eV}$, $t_\perp = 0.1t$, $V_g = 0.03t$, $a = 1.42\text{\AA}$, and $W = 160$ (in units of number of atomic layers; inter-edge scattering is negligible with this width).

Acknowledgements This work has been supported by the Swiss National Science Foundation (projects 200020-121807, 200021-121569) and by the Swiss Center of Excellence MaNEP. The work of IM was carried out under the auspices of the National Nuclear Security Administration of the U.S. Department of Energy at Los Alamos National Laboratory under Contract No. DE-AC52-06NA25396 and supported by the LANL/LDRD Program.

-
- [1] Son, Y., Cohen, M. L. & Louie, S. G. Half-metallic graphene nanoribbons. *Nature* **444**, 347–349 (2006).
- [2] Rycerz, A., Tworzydło, J. & Beenakker, C. W. J. Valley filter and valley valve in graphene. *Nature Phys.* **3**, 172–175 (2007).
- [3] Guinea, F., Katsnelson, M. I. & Geim, A. K. Energy gaps and a zero-field quantum Hall effect in graphene by strain engineering. *Nature Phys.* **6**, 30–33 (2010).
- [4] Oostinga, J. B., Heersche, H. B., Liu, X., Morpurgo, A. F. & Vandersypen, L. M. K. Gate-induced insulating state in bilayer graphene devices. *Nature Mater.* **7**, 151–157 (2008).
- [5] Zhang, Y. *et al.* Direct observation of a widely tunable bandgap in bilayer graphene. *Nature* **459**, 820–823 (2009).
- [6] Mak, K. F., Lui, C. H., Shan, J. & Heinz, T. F. Observation of an electric-field-induced band gap in bilayer graphene by infrared spectroscopy. *Phys. Rev. Lett.* **102**, 256405 (2009).
- [7] Novoselov, K. S. *et al.* Two-dimensional gas of massless Dirac fermions in graphene. *Nature* **438**, 197–200 (2005).
- [8] Zhang, Y., Tan, Y., Stormer, H. L. & Kim, P. Experimental observation of the quantum Hall effect and Berry’s phase in graphene. *Nature* **438**, 201–204 (2005).
- [9] Novoselov, K. S. *et al.* Unconventional quantum Hall effect and Berry’s phase of 2π in bilayer graphene. *Nature Phys.* **2**, 177–180 (2006).
- [10] Nakada, K., Fujita, M., Dresselhaus, G. & Dresselhaus, M. S. Edge state in graphene ribbons: Nanometer size effect and edge shape dependence. *Phys. Rev. B* **54**, 17954 (1996).
- [11] Castro, E. V., Peres, N. M. R., dos Santos, J. M. B. L., Neto, A. H. C. & Guinea, F. Localized states at zigzag edges of bilayer graphene. *Phys. Rev. Lett.* **100**, 026802–4 (2008).
- [12] Yao, W., Yang, S. A. & Niu, Q. Edge states in graphene: From gapped flat-band to gapless chiral modes. *Phys. Rev. Lett.* **102**, 096801–4 (2009).
- [13] Brey, L. & Fertig, H. A. Electronic states of graphene nanoribbons studied with the Dirac equation. *Phys. Rev. B* **73**, 235411–5 (2006).
- [14] McCann, E. & Fal’ko, V. I. Landau-level degeneracy and quantum Hall effect in a graphite bilayer. *Phys. Rev. Lett.* **96**, 086805–4 (2006).
- [15] Volovik, G. *The Universe in a Helium Droplet* (Oxford University Press, 2003).

- [16] Martin, I., Blanter, Y. M. & Morpurgo, A. F. Topological confinement in bilayer graphene. *Phys. Rev. Lett.* **100**, 036804–4 (2008).
- [17] Qi, X., Hughes, T. L. & Zhang, S. Topological field theory of time-reversal invariant insulators. *Phys. Rev. B* **78**, 195424–43 (2008).
- [18] Hasan, M. Z. & Kane, C. L. Topological insulators. Preprint at <<http://arxiv.org/abs/1002.3895>> (2010).
- [19] Kane, C. L. & Mele, E. J. Quantum spin Hall effect in graphene. *Phys. Rev. Lett.* **95**, 226801 (2005).
- [20] Kane, C. L. & Mele, E. J. Z₂ topological order and the quantum spin Hall effect. *Phys. Rev. Lett.* **95**, 146802 (2005).
- [21] Bernevig, B. A., Hughes, T. L. & Zhang, S. Quantum spin Hall effect and topological phase transition in HgTe quantum wells. *Science* **314**, 1757–1761 (2006).
- [22] König, M. *et al.* Quantum spin Hall insulator state in HgTe quantum wells. *Science* **318**, 766–770 (2007).
- [23] Roth, A. *et al.* Nonlocal transport in the quantum spin Hall state. *Science* **325**, 294–297 (2009).
- [24] Mucciolo, E. R., Neto, A. H. C. & Lewenkopf, C. H. Conductance quantization and transport gaps in disordered graphene nanoribbons. *Phys. Rev. B* **79**, 075407–5 (2009).
- [25] Martin, J. *et al.* Observation of electron-hole puddles in graphene using a scanning single-electron transistor. *Nature Phys.* **4**, 144–148 (2008).
- [26] Kuzmenko, A. B., Crassee, I., van der Marel, D., Blake, P. & Novoselov, K. S. Determination of the gate-tunable band gap and tight-binding parameters in bilayer graphene using infrared spectroscopy. *Phys. Rev. B* **80**, 165406 (2009).
- [27] Allen, M., Weitz, T., Martin, J., Feldman, B. & Yacoby, A. Tunable energy gap in suspended bilayer graphene. APS March Meeting 2010 presentation, P22.00002 (2010).

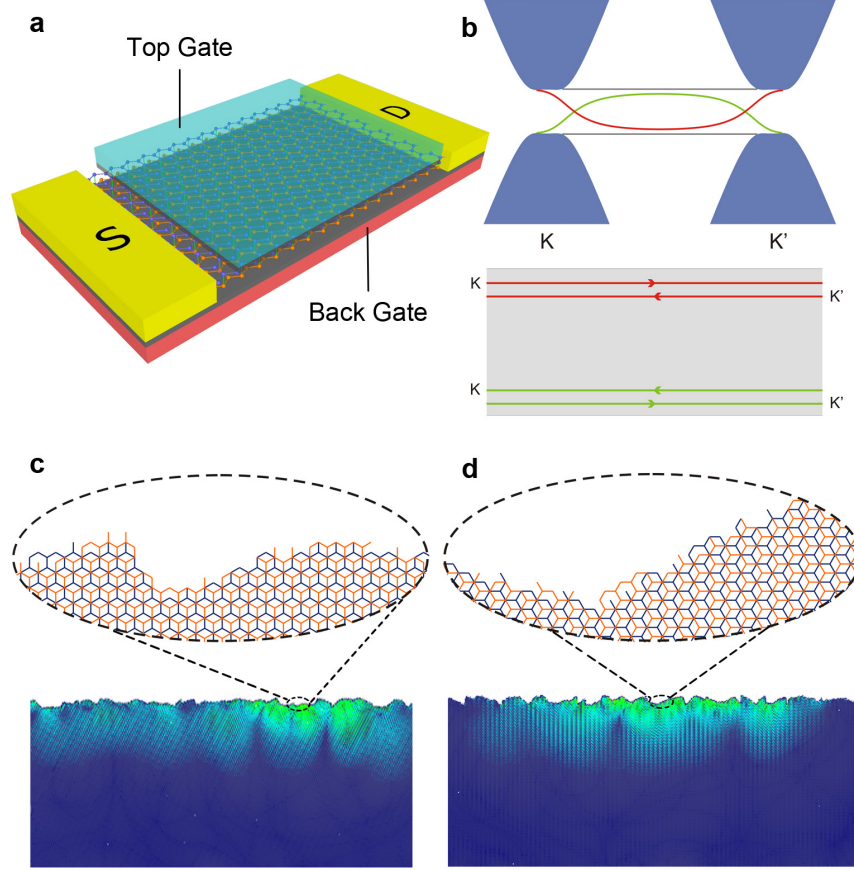


FIG. 1: Edge states in gapped BLG. Panel **a** shows a schematic view of the device. By controlling the gate voltages applied to the top and back gates separately, an energy gap in the bulk of BLG can be opened and tuned, while maintaining the Fermi energy in its center. Panel **b** shows the dispersion of the sub-gap edge states in gapped BLG at a zig-zag edge. At both edges, the states are helical with respect to the valley degree of freedom, with states in opposite valleys propagating in opposite directions. This conclusion holds for periodic edges of rather general shape (i.e. not only for zig-zag), but it does not hold for the ideal armchair edge, where two valleys (K and K') are fully coupled and no sub-gap edge states are present. Panels **c** and **d** show the typical probability density near zero energy for strongly disordered BLG zig-zag (**c**) or armchair (**d**) edges. In the presence of realistically strong disorder, the existence of such edge states – and their long localization length – is a universal property of gapped BLG (the panels correspond to a BLG that is approximately 100 nm long).

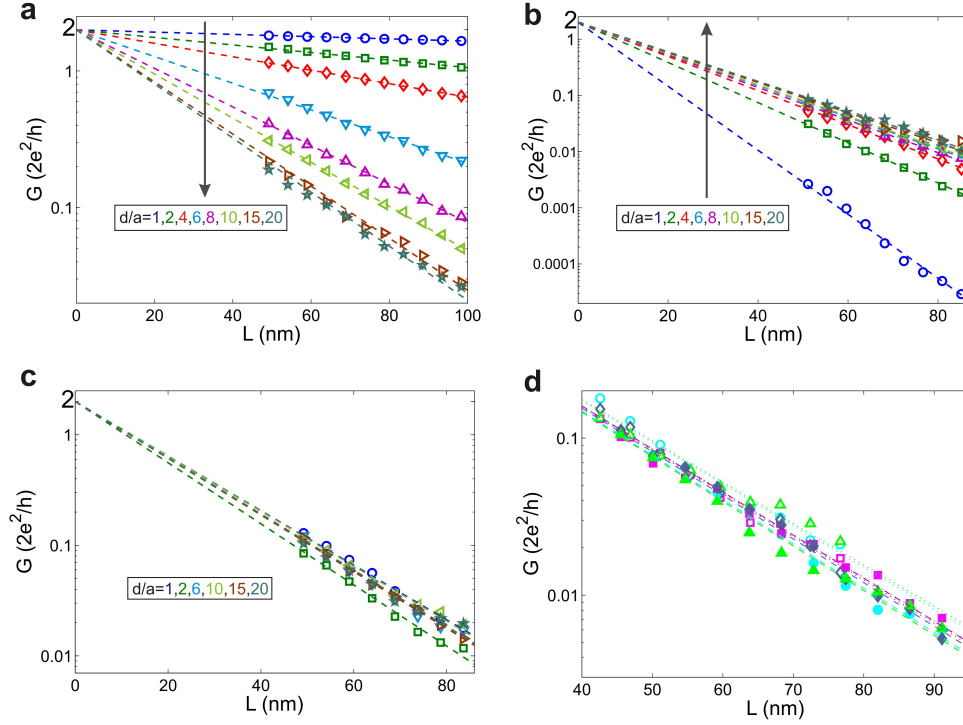


FIG. 2: Subgap conductance in disordered BLG. Panels **a-d** show the decay of average conductance G (at $E_f = 0$) with increasing length L of the BLG strips, for different amounts of disorder. In panel **a** and **b**, the arrows indicate that the evolution of the conductance with increasing structural edge roughness (quantified by the edge roughness depth d) is opposite for samples starting from ideal zig-zag (**a**) and armchair (**b**) edges. The functional dependencies of the conductance as a function of L calculated for different values of d converge to the same universal limit when disorder is sufficiently strong (i.e., the $G(L)$ traces become universal at large d). Panel **c** shows that in the presence of “chemical” disorder –consisting of random on-site energies for the outermost tight-binding sites, distributed between ± 1 eV– the $G(L)$ traces become rather insensitive to the value of d (i.e., chemical disorder or large structural disorder have identical effects; the data shown in the panel are obtained starting from an ideal zig-zag edge). Panel **d** further shows the comparison of $G(L)$ traces calculated in the presence of strong disorder (in the universal limit) starting from armchair edges and for another crystallographic edge obtained by cutting the BLG edge at a $\theta \approx 10.9^\circ$ angle from the armchair direction (calculations were performed with $d = 20a$). It is apparent that the results are virtually identical, confirming once again that for strong disorder different orientations become equivalent. The data shown in panel **d** have been calculated for samples of different width W (in units of number of atomic layers: circles correspond to $W = 160$, squares to $W = 200$, diamonds to $W = 240$, triangles to $W = 280$): the lack of sensitivity to W indicates that sub-gap transport is dominated by edge states and not by the BLG bulk. The fact that transport is occurring at the edges can also be inferred from the data of panels **a-c**, that show that the conductance extrapolates in all cases to $G \rightarrow 2$ (in units of $2e^2/h$) in the limit $L \rightarrow 0$ (corresponding to one spin degenerate edge channel at each sample edge).

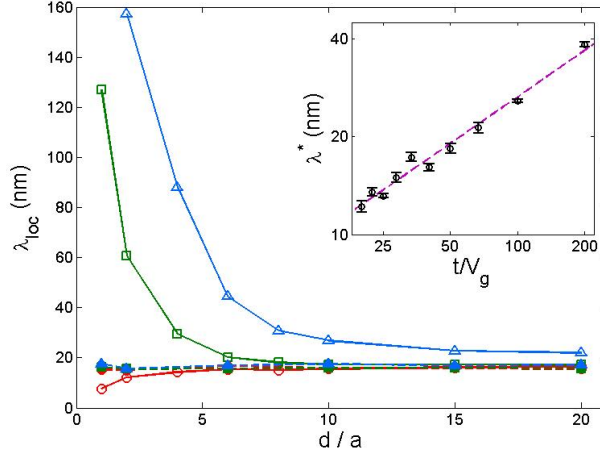


FIG. 3: **Universal behavior of localized edge states.** The figure shows the dependence of the localization length λ_{loc} on the amount of edge disorder, for the different orientations of the ideal “starting” edges (the data are extracted from plots similar to those shown in Fig.2: circles correspond to armchair edges, squares to a direction cut at a $\theta \approx 10.9^\circ$ angle from the armchair direction, triangles to zig-zag edges). The cases in which only structural disorder is considered – quantified by the roughness depth d – correspond to the data points connected by solid lines. In those cases λ_{loc} depends on both d and θ , until it saturates at large d . The cases in which strong “chemical” disorder is also included, modeled by random on site energies on the outermost row of carbon atoms, correspond to the data points connected by the broken line. With chemical disorder, the “universal” value of the localization length is reached already for very small structural disorder (i.e. $d \simeq 1$). In all cases, sufficiently strong disorder leads to the same value of λ_{loc} regardless of any details. This demonstrates that, for sufficiently strong disorder, the localization length of the edge states is universal, and depends only on the magnitude of the band-gap V_g . The universal value of λ_{loc} for different values of the gap V_g is shown in the inset. We find that λ_{loc} is approximately proportional to $1/\sqrt{V_g}$ (see the log-log plot in the inset; the line is a fit yielding $\lambda_{loc} \propto 1/V_g^\nu$ with $\nu = 0.48 \pm 0.06$).

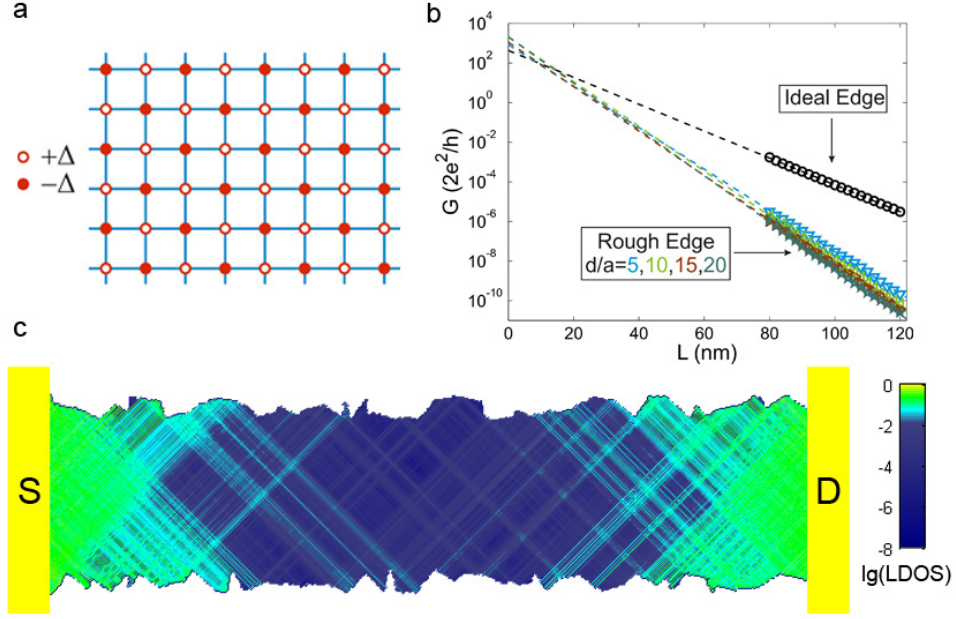


FIG. 4: **Absence of disorder-induced edge transport in a topologically trivial system.**

As a term of comparison for gapped BLG, we analyze sub-gap transport in a square lattice, with a staggered potential Δ that determines the size of the gap, equal to 2Δ (see panel **a**; the lattice constant a is set to $a = 1\text{\AA}$). Sub-gap transport is investigated by setting the Fermi energy at the center of the gap. Panel **b** shows the subgap conductance G as a function of strip length L , for the ideal edge, and for edges with different amount of structural disorder. In this case edge roughness significantly lowers the conductance as compared to the case of ideal edges. In all cases, transport occurs through the bulk of the system and is due to evanescent modes decaying from the source and drain contacts (S and D in panel **c**), i.e. it is due to tunneling through the bulk gap. This is why, contrary to gapped BLG, the conductance extrapolates to large values when $L \rightarrow 0$. Panel **c** shows the local density of states in a rough-edge sample 60 nm long. The scar-like trajectories in the bulk are caused by edge disorder, which affect the evanescent waves that decay exponentially away from the contacts. No evidence of edge states is found in this system.